GSA DATA REPOSITORY 2018105

Polar desert chronologies through quantitative measurements of salt accumulation

Joseph A. Graly[1], Kathy J. Licht[1], Gregory K. Druschel[1], and Michael R. Kaplan[2]
[1]Department of Earth Sciences, IUPUI, Indianapolis, Indiana 46202, USA
[2]Lamont–Doherty Earth Observatory, Palisades, New York 10964, USA

https://doi.org/10.1130/G39650.1

Appendix DR1: **Chemical Results**

Table DR1 summarizes the data that underlies the manuscript. Some additional measurements were also performed to test the reliability and precision of the analytical methods. For a small number of samples (1A,2A,3A,3D,4C,4F; n = 6), a second 24 h leach was performed to test whether complete salt dissolution had occurred during the earlier leach. In all cases, the concentration of sulfur in this second leach was less than 1 µmol per g sediment, suggesting complete dissolution of sulfate in the initial round. For a single sample (4C), three separate aliquots were independently extracted. The ICP-OES results are within 5% of the average concentration for each measured element. The proportion of each element varies within 1% of average proportion, implying that most the variation is in total concentration not in the relative abundance of individual elements. Root mean squared errors for the triplicate measurements of the ICP-OES are typically <1%.

Table DR1: Analytic Chemical Results. Errors generally <1% of measured value. NO_2, PO_4, and Br were at undetectable levels in all samples

Sample	Year Sampled	Latitude	Longitude	Distance (m)	Exposure Age (isotope kyrs)**	Elements on ICP-OES (µmol per g sediment)					Anions on IC (µmol per g)			
						Na	K	Ca	Mg	B	Fl^-	Cl^-	NO_3^-	SO_4^{2-}
1A	2010	-84.183	161.268	121	-	1.63	0.81	5.47	0.44	0.11	0.60	1.00	<0.2	1.82
1B	2010	(adjacent to 1A)		122	-	1.75	0.98	4.51	0.64	0.11	<0.1	4.43	0.97	0.66
1C	2010	-84.178	161.537	150	^{3}He 6.7 ± 0.6	6.69	0.80	2.88	0.48	0.13	0.86	4.90	1.30	1.44
1A Crest 2	2015	-84.185	161.273	381	-	2.60	0.86	4.09	0.62	0.22	<0.1	1.51	0.48	1.66
2C	2015	-84.187	161.276	566	^{3}He 11.4 ± 0.7	15.70	1.14	5.78	1.15	0.24	<0.1	0.84	2.60	11.23
2B	2015	-84.187	161.242	656	-	40.71	0.85	6.68	1.70	0.34	3.21	1.29	10.10	20.23
2A	2010	-84.188	161.268	712	^{10}Be 14.0 ± 0.4	21.51	1.38	21.79	2.28	0.19	1.80	11.03	6.27	29.77
3C	2010	-84.191	161.282	1021	^{10}Be 6.0 ± 0.3	13.51	1.78	31.59	3.85	0.15	1.58	8.05	5.85	31.29
3D	2010	-84.191	161.280	1038	-	14.57	1.73	26.31	2.32	0.14	1.30	8.28	4.08	28.49
3Dark*	2010	-84.192	161.288	1218	-	7.15	1.49	7.17	0.70	0.12	<0.1	4.41	2.14	3.17
3B	2010	-84.193	161.288	1262	-	19.21	1.61	27.82	2.95	0.23	1.66	6.20	5.63	29.18
3A	2010	-84.193	161.288	1288	-	21.48	2.64	40.37	4.95	0.19	1.95	13.16	8.22	38.66
3E	2010	-84.195	161.279	1472	-	19.30	1.41	54.31	3.87	0.18	1.05	9.66	6.76	61.42
4O	2015	-84.197	161.259	1680	-	6.73	1.00	3.54	0.60	0.12	0.16	1.96	0.95	0.84
3F Bottom	2015	-84.197	161.312	1788	-	11.45	1.03	10.93	1.65	0.10	1.55	4.15	4.59	7.47
3F Top	2015	-84.197	161.312	1788	-	16.67	0.96	14.88	3.75	0.31	1.16	3.47	3.98	28.44
4N	2015	-84.198	161.263	1810	^{10}Be 52.3 ± 1.7	23.30	1.46	9.81	1.04	0.43	0.22	4.35	4.19	17.17
4M Bottom	2015	-84.200	161.292	2015	-	15.38	1.54	13.81	1.24	<0.1	0.29	14.64	7.77	3.85
4M Top	2015	-84.200	161.292	2015	^{10}Be 104.9 ± 2.7	29.58	2.47	26.62	5.73	0.70	1.79	15.33	10.40	32.35
4L	2010	-84.202	161.327	2313	-	93.37	1.67	80.07	8.40	0.69	2.95	43.69	8.61	70.51
4K	2010	-84.202	161.330	2393	-	65.19	1.41	62.54	6.89	0.57	2.56	35.77	20.19	125.27
4J	2010	-84.202	161.328	2409	-	48.70	1.36	76.51	4.17	0.63	2.27	38.08	18.86	64.56
4I	2010	-84.205	161.351	2742	-	89.40	1.73	119.75	17.95	0.72	5.93	25.61	23.92	146.59
4G	2010	-84.209	161.367	3245	^{10}Be 184.6 ± 5.0	170.86	2.38	129.09	18.16	1.06	8.06	56.75	36.18	174.52
4H*	2010	-84.209	161.367	3270	-	122.78	1.73	99.80	14.06	0.50	3.45	39.23	22.52	123.44
4F	2010	-84.214	161.367	3749	-	180.65	1.28	50.59	8.45	1.77	12.73	56.92	19.16	90.66
4E	2010	-84.216	161.364	3990	-	229.00	2.35	183.75	24.97	2.10	6.44	70.26	64.61	277.46
4D	2010	-84.218	161.361	4231	-	250.60	1.08	55.34	9.02	2.97	18.41	79.45	20.62	132.15
4P	2015	-84.219	161.338	4290	^{10}Be 552.4 ± 15.4	399.33	3.62	112.78	36.88	3.61	4.76	94.58	126.40	236.11
4C	2010	-84.219	161.361	4305	-	157.22	2.60	138.68	16.24	1.03	5.61	40.99	38.28	145.37
4Q	2015	-84.221	161.342	4501	-	71.10	2.57	79.94	24.29	1.90	0.51	32.84	50.00	95.57
4B	2010	-84.222	161.358	4582	^{10}Be 191.3 ± 5.2	180.49	1.67	99.22	14.11	1.13	6.28	62.76	36.26	116.99
4A	2010	-84.223	161.356	4714	-	121.23	1.44	90.81	10.55	0.78	4.56	43.82	22.85	130.67
5A	2010	-84.226	161.274	4941	^{3}He 105.1 ± 2.9	146.69	1.27	142.71	14.88	0.74	6.00	35.77	20.57	88.03
5B	2010	-84.229	161.273	5234	^{3}He 304.6 ± 7.1	168.23	1.55	115.49	18.96	1.94	6.26	53.09	30.69	175.27
5E	2010	-84.230	161.305	5394	-	307.36	2.15	218.70	28.91	2.59	7.99	96.08	79.45	344.75
5C	2010	-84.232	161.274	5628	-	575.54	2.50	56.70	19.27	4.87	31.00	508.34	40.57	169.54
5D	2010	-84.236	161.281	6081	-	446.89	3.32	279.64	45.10	7.49	15.93	701.71	73.15	108.84

* Trough Bottom Sample

**For complete data see Kalpan et al., 2017

Appendix DR2**: Comparison of upper and lower sections of soil profiles along with geochemical modeling**

In two locations, we collected both samples of the topsoil and a second sample below a distinct oxidation horizon at ~5 cm depth, where the soil changes from light grey to dark or very dark grey, respectively (Figure DR1). Across the Mt. Achernar moraine, nine soil pits were also independently sampled by Scarrow and others (2014) with 2 to 4 samples per pit at various depths. Their efforts were ~2 km to the west of our transect, closer to the Mt. Achernar headwall (Figure 1) and used whole samples rather than the fine fraction. We include their data below, contrasting samples collected above and below oxidative weathering horizons that are similar to those featured in Figure DR1. In three locations, we collected samples in adjoining ridges and troughs. The troughs typically have a substantially thinner soil mantle over the ice, suggesting the sediment is actively fluxing predominantly to the ridges. The results of comparing bottom soil to top soil and troughs to ridges are in Table DR2 below, using both data from this study and from the Scarrow et al. study.

Table DR2: Ratios of anion concentrations between top and bottom soils or adjoining troughs and ridges

Type	Sample	Distance (m)	Depth (cm)	Ratio of Bottom to Top Concentrations				
				B	Cl	NO_3^-	SO_4^{2-}	Total
Bottom Soil	3F	1788	4	0.16	1.20	1.15	0.26	0.39
Bottom Soil	4M	2015	5	<0.35	0.96	0.75	0.12	0.33
Bottom Soil*	NA	550	5	NA	1.61	1.07	0.25	0.47
Bottom Soil*	NA	800	4.5	NA	0.73	0.22	0.24	0.28
Bottom Soil*	NA	1500	8.5	NA	0.45	0.34	0.48	0.47
Bottom Soil*	NA	2200	36.5	NA	0.98	0.86	0.19	0.23
Bottom Soil*	NA	2900	16	NA	2.65	2.96	0.40	0.50
Bottom Soil*	NA	3600	37.5	NA	0.85	0.69	0.51	0.53
Bottom Soil*	NA	4200	32.5	NA	1.45	0.55	0.75	0.74
Bottom Soil*	NA	5300	34.5	NA	1.66	1.24	0.85	0.93
Bottom Soil*	NA	5500	30.5	NA	1.84	0.41	0.16	0.31
Soil Average		-	-	NA	1.31	0.93	0.38	0.47
Trough	3Dark:3B	1098	NA	0.26	0.71	0.38	0.11	0.18
Trough	4O:4N	1560	NA	0.26	0.45	0.23	0.05	0.11
Trough	4H:4G	3125	NA	0.47	0.69	0.62	0.71	0.69

*Data from Scarrow et al., 2014

Sulfate is substantially depleted below the oxidative weathering horizon, in most cases far more so than the total difference in ionic strength. Chloride is generally not depleted below the oxidation horizon and, in many cases, is enriched at depth. Though there is large variance in the change in nitrate concentrations across the oxidation horizon, on average, depletion is minimal. When comparing troughs to adjacent ridges, similar patterns hold in the two younger trough samples (listed first), in which trough soils are < 10 cm deep. This is likely because chloride and nitrate have fluxed to depth in the corresponding ridge, but do not have sufficient space to do so in the thinly-mantled trough.

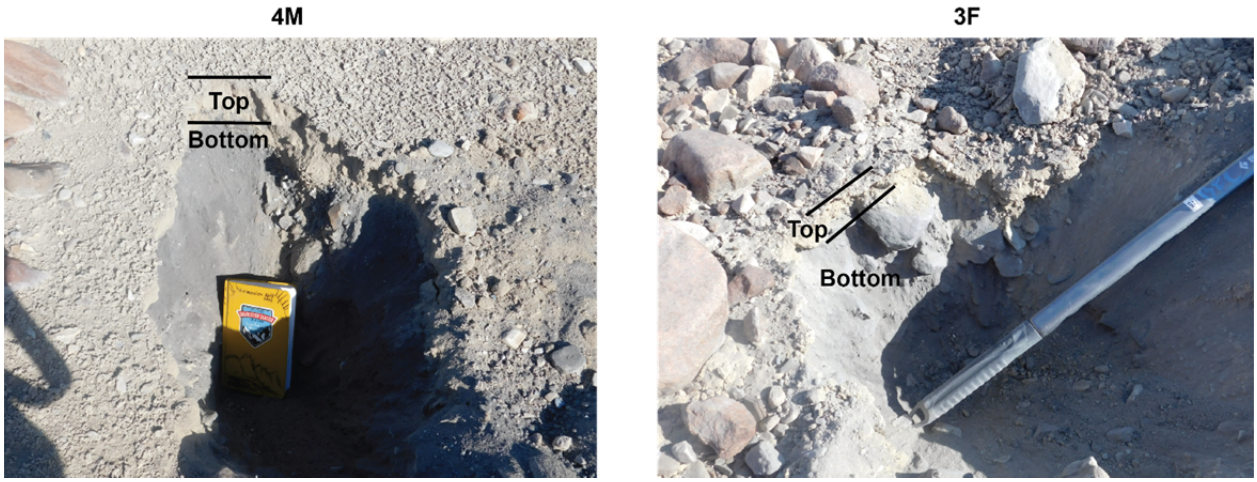

Figure DR1. Oxidation horizons in samples 4M and 3F

In order to examine the possible processes by which salt is transported to depth, we used The Geochemist's Workbench Pro (v. 9.0) software to simulate the solubility of the salt minerals present at the analyzed top soil samples. The thermodynamic constants for the minerals were taken from Anovitz and Hemingway (1996), Wang and others (2016), and the built in thermodynamic database of the software package (thermo.dat). Our initial condition consisted of the constituents of sample 4e dissolved into 10 ml of water. To simulate the water's evaporation, we had the software progressively titrate in the ions for sample 4e (Table DR1). This allows us to model the relative salt solubility with in the soil column as ionic concentrations rise due to evaporative concentration (x-axis records increasing evaporation left to right, plotted as reaction progress in Figure DR2). The results of the model outcome suggest that both nitrate and sulfate should be highly immobile and borate and chloride should be highly mobile in a flow through porous media setting. Contrastingly, the data suggest that nitrate and chloride are mobile, whereas boron and sulfate are immobile (Table DR2). These results support our suggestion that vapor phase effects are primarily responsible for the downward mobility of salts (through vapors of associated acids).

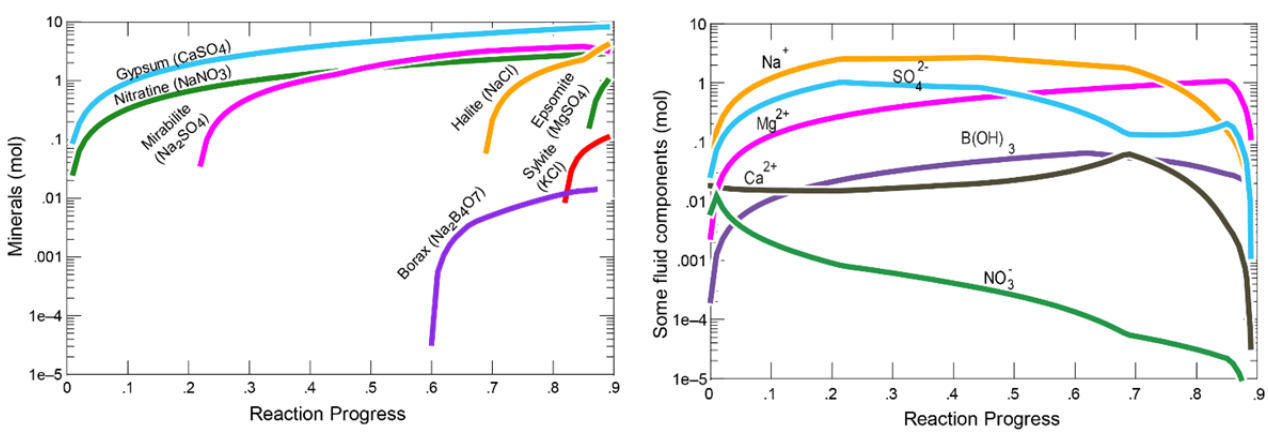

Figure DR2: Model run of mineral precipitation in a drying solution that contains initial constituents similar to the salts found in the well-developed top soil samples.

Appendix DR3: **Comparison of estimated aerosol fallout rates to aerosol flux in Antarctic ice cores**

In order to determine whether salts are primarily derived from aerosols and whether they are consistently retained in soils, it is useful to compare the flux of salts to the moraine sediments to the flux of aerosols in Antarctic ice cores. Because the aerosols in ice cores have a solely atmospheric origin, comparisons to sediment establishes to first order, whether atmospheric deposition of aerosols is primarily responsible for salt accumulation on the moraine.

Prior to comparing them ice cores, we estimated of the average annual flux of aerosol salts to the moraine sediments. The estimation is complicated by the fact that most samples are only characterized by a single sample from the top layer of the soil profile, of which only the finest grain size fraction was analyzed. In cases where a soil sample was collected at depth, a substantial drop in borate and sulfate is documented (Table DR2), but the depth and shape of the decline is not. We can nevertheless make first order estimates of the aerosol flux. Assuming aerosol fallout is linear over timescales of moraine formation (as is suggested by ice core records), a linear relationship between anion concentration in the measured top layer of the soil requires that this layer retain an approximately consistent percentage of the total anion load. Inasmuch as this percentage can be estimated, an average annual flux can be inferred.

In the younger (<50,000 year) sediment, our pits reached exposed ablating glacial ice beneath the sediment. In these samples, a linear correlation is found between the depth to ice and the surface exposure ages inferred from the correlation of boron concentrations to cosmogenic nuclide exposure ages (Figure DR3). This correlation implies a sediment generation rate of $6.9*10^{-4}$ cm per year. Assuming a density of ~1.5 g per cm^3, this relationship implies ~10 g of sediment ablate out of the moraine per m^2 per year. It appears that above a certain sediment thickness, this sediment generation rate is substantially greater than the rate at which an oxidative weathering front can advance through the sediment. The youngest samples (<10^4 year) are only partially oxidized, retaining a grey color. In intermediate-aged soils (10^4 to 10^5 year) a distinct oxidized layer emerges in the first ~5 cm, with grey soil continuing below. In older (>10^5 year) soils, oxidized soil continued through the top tens of cm of the soil. In the intermediate-aged soils, samples above this horizon were enriched in sulfate and borate several fold compared to those below, but had comparable levels of chloride and nitrate (Table DR2).

Because sulfate is confined to the thin oxidized layer, we can approximately constrain the distribution of sulfate in the soil (whereas attempts to constrain the other major anions would be pure guess work). If we then assume that sulfate deposition was confined at first order to the top 4-5 cm, and assume that our measurements captured the average sulfate concentration of this top layer, we can use this thickness to estimate total fallout. We find a linear increase of $7.66*10^{-4}$ µmoles sulfate per gram per year over the first 200 ka of the cosmogenic isotope record (Fig. 2).

The salt concentration measurements were only taken on the <63 µm grain size fractions. The fraction of our samples that are silt and clay size is 27 ± 10% (Bader et al., 2017). Surface area effects suggest that most of the salts will be in this fraction. Furthermore, Scarrow et al. (2014) measured salt concentrations from whole sediment samples and derived concentrations ~ 4 times lower than ours. We therefore divide by 4 to correct for grain size distribution. A sulfate horizon thickness of 5 cm (and the other factors above) produce a sulfate fallout of 14.4 µmoles per m^2 per year; 4 cm gives 11.5 $\mu mol \cdot m^{-2} a^{-1}$. While this result should be taken as first order approximation, it is approximately a factor of 2 lower than sulfate fluxes to interior Antarctic ice cores, including EPICA (Wolff et al., 2010), Vostok (Legrand et al., 1988), and Dome Fuji (Ohno et al., 2006).

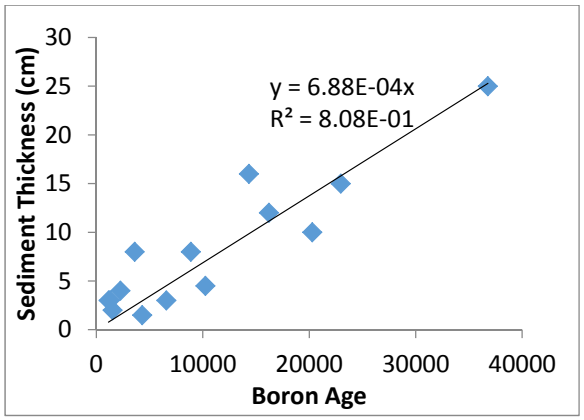

Figure DR3: Depth to ice in young soils compared to the soil age implied by the linear correlation between boron concentration and cosmogenic-nuclide exposure age (Fig. 2). Errors within symbol size.

The nearest ice core to the Mt. Achernar site is the Dominion Range ice core, ~100 km away and also located in the interior-most Transantarctic Mountains. Ice chemical measurements were performed on the core, and though formal accumulation rate measurements are absent, we can estimate them from the ice depth over which the Holocene and last glacial maximum occur (Mayewski et al., 1990). Compared to other Antarctic ice cores (e.g. Watanabe et al., 1999), Holocene accumulation of around 1 cm ice per year are suggested for the Dominion Range ice core. Pleistocene accumulations are comparably around 3/5ths of this value. Using these accumulation rates, the measured sulfate concentrations in the Dominion Range ice core produce sulfate fallouts of 10.5 ± 1.9 $\mu mol \cdot m^{-2} a^{-1}$ for the Holocene (based on 1358 measurements) and ~17 $\mu mol \cdot m^{-2} a^{-1}$ for the last glacial maximum (based on 2 measurements). These results are consistent with our estimates of soil sulfate content within Mt. Achernar moraine.

Sulfate flux to ice cores is typically consistent between glacial and interglacial periods (e.g. IIzuka et al., 2012). Contrastingly, chloride and nitrate fluxes are elevated by a factor of 2 to 5 in Pleistocene sections of ice cores. If fallout to the moraine soils follows the same pattern, we would expect to see slower rates of nitrate and chloride accumulation in interglacial periods. However, the opposite is observed in the soil data, with the Holocene aged samples having concentrations of nitrate and chloride that plot above the regression line between the individual anions and cosmogenic exposure age (Fig. 2). This can be explained by the fact that nitrates and chlorides are fluxed to greater depth within the soil profile. If the depth of sediment to which the anions are fluxed has not yet developed in the moraine, concentrations of those anions will be elevated in the sediment that has emerged. In cases where less developed soil samples were collected from the thinly mantled intermorainal troughs, relatively elevated nitrate and chloride concentrations are also observed (Table DR2).

Data Repository References

Anovitz, L.M. and Hemingway, B.S. (1996) Thermodynamics of boron minerals; summary of structural, volumetric and thermochemical data. Reviews in Mineralogy and Geochemistry 33, 181-261.

Bader, N.A., Licht, K.J., Kaplan, M.R., Kassab, C. and Winckler, G. (2017) East Antarctic ice sheet stability recorded in a high-elevation ice-cored moraine. Quaternary Science Reviews 159, 88-102.

IIzuka, Y., Uemura, R., Motoyama, H., Suzuki, T., Miyake, T., Hirabayahsi, M. and Hondoh, T. (2012) Sulphate–climate coupling over the past 300,000 years in inland Antarctica. Nature 490, 81-84.

Kaplan, M.R., Licht, K.J., Winckler, G., Schaefer, J.M., Bader, N., Mathieson, C., Roberts, M., Kassab, C.M., Schwartz, R. and Graly, J.A. (2017) Mid-Late Pleistocene stability of the central East Antarctic Ice Sheet at the head of Law Glacier. Geology, accepted manuscript.

Legrand, M.R., Lorius, C., Barkov, N.I. and Petrov, V.N. (1988) Vostok (Antarctica ice core: Atmospheric chemistry changes over hte last climatic cylce (160,000) years. Atmospheric Environment 22, 317-331.

Mayewski, P.A., Twickler, M.S., Lyons, W.B. and Spencer, M.J. (1990) The Dominion Range Ice Core, Queen Maud Mountains, Antarctica - General site and core characteristics with implications. Journal of Glaciology 36, 11-16.

Ohno, H., Igarashi, M. and Hondoh, T. (2006) Characteristics of salt inclusions in polar ice from Dome Fuji, East Antarctica. Geophysical Research Letters 33, L08501.

Scarrow, J.W., Balks, M.R. and Almond, P.C. (2014) Three soil chronosequences in recessional glacial deposits near the polar plateau, in the Central Transantarctic Mountains, Antarctica. Antarctic Science 26, 573-583.

Wang, M., Gorensek, M.B. and Chen, C.-C. (2016) Thermodynamic representation of aqueous sodium nitrate and nitric acid solution with electrolyte NRTL model. Fluid Phase Equilibria 407, 105-116.

Watanabe, O., Kamiyama, K., Motoyama, H., Fujii, Y., Shoji, H. and Satow, K. (1999) The paleoclimate record in the ice core at Dome Fuji station, East Antarctica. Annals of Glaciology 29, 176-178.

Wolff, E.W., Barbante, C., Becagli, S., Bigler, M., Boutron, C.F., Castellano, E., de Angelis, M., Federer, U., Fischer, H., Fundel, F., Hansson, M., Hutterli, M., Jonsell, U., Karlin, T., Kaufmann, P., Lambert, F., Littot, G.C., Mulvaney, R., Röthlisberger, R., Ruth, U., Severi, M., Siggaard-Andersen, M.L., Sime, L.C., Steffensen, J.P., Stocker, T.F., Traversi, R., Twarloh, B., Udisti, R., Wagenbach, D. and Wegner, A. (2010) Changes in environment over the last 800,000 years from chemical analysis of the EPICA Dome C ice core. Quaternary Science Reviews 29, 285-295.